ELSEVIER

Polymer 41 (2000) 8839–8848

polymer

www.elsevier.nl/locate/polymer

Steps in the formation of the partially crystalline state

B. Heck, T. Hugel, M. Iijima, G. Strobl*

Fakultät für Physik der Albert-Ludwigs-Universitat, 79104 Freiburg, Germany

Received 4 October 1999; received in revised form 20 January 2000; accepted 5 February 2000

Abstract

Time- and temperature-dependent SAXS studies carried out on s-polypropylene, various s-poly(propene-*co*-octene)s, two poly(ethylene-*co*-octene)s and poly(-caprolactone) indicate that the transition from the entangled melt to the partially crystalline state occurs generally in two steps. At first, an initial form of lower order builds up which then becomes stabilized to end in the final state with lamellar morphology. AFM observations suggest that the initial structure is composed of crystal blocks in planar assemblies, which then fuse into a homogeneous lamella. The edge length of the blocks in chain direction determines also the lamellar thickness. The size of the blocks corresponds to the minimum necessary to be stable. The crystallinities after isothermal crystallization processes remain invariant over larger temperature ranges, thus demonstrating that the potential of the entangled melt to form crystals is a well-defined property.

Keywords: Polymer crystallization; Small angle X-ray scattering; AFM

1. Introduction

1.1. Crystallization and melting of syndiotactic polypropylene

Time- and temperature dependent SAXS experiments carried out on syndiotactic polypropylene and various s-poly(propene-*co*-octene)s provided us with a detailed, accurate picture of the relations between the crystallization temperature T_c, the crystal thickness d_c and the location of the melting peak T_f. In particular, the effects introduced by the presence of the co-units, which cannot be included in the crystallites, were clearly indicated [1]. Fig. 1 gives a typical example and demonstrates some important properties. It refers to the copolymer with 4% per weight of octene units and depicts in a combined manner both the evolution of the interface distance distribution function during an isothermal crystallization at 125°C and the changes during a subsequent heating up to the melt. The dominant feature is the peak located at 6.5 nm which relates to the crystallites and gives their thickness d_c. As can be seen, its location remains constant, i.e. there is no solid-state thickening during the crystallization. Even more important, also the melting which starts immediately above T_c is not accompanied by a change in d_c. Hence, there are more controlling factors for the crystal stability than just d_c. Fig. 2 collects the data derived from such experiments for all samples. The four parallel lines give the relation between the melting peak and the crystal thickness for the different samples, plotting T_f versus d_c^{-1} as suggested by the Gibbs–Thomson relation. One observes as expected a shift to lower temperatures with increasing co-unit content. The other line with the higher slope, the 'crystallization line', represents the relation T_c versus d_c^{-1}. One observes a linear relation, and surprisingly, no effect at all from the co-units; the thicknesses of all samples are on one common line. We also measured DSC thermograms for all samples and Fig. 3 gives a selection. Heating always occurred immediately after an isothermal crystallization, in correspondence to the SAXS experiments. Melting begins a couple of degrees above T_c, then increases and reaches a maximum at T_f. One observes a certain tendency when varying the content of octene units. An increase leads to a more continuous appearance of the thermograms, and for the higher co-unit contents finally to the evolution of a second peak near to T_c. The latter curves may be addressed as showing the melting of two groups of crystallites with different stability. This difference, however, is *not* based on a difference in d_c, as is demonstrated by the SAXS experiments.

Observations may be understood as evidence that the building-up of the lamellar crystallites is a two-step process. The crystallization line relates to a first imperfect form, which then changes into the lamellar crystallites melting

* Corresponding author.
E-mail address: strobl@uni-freiburg.de (G. Strobl).

0032-3861/00/$ - see front matter
PII: S0032-3861(00)00227-5

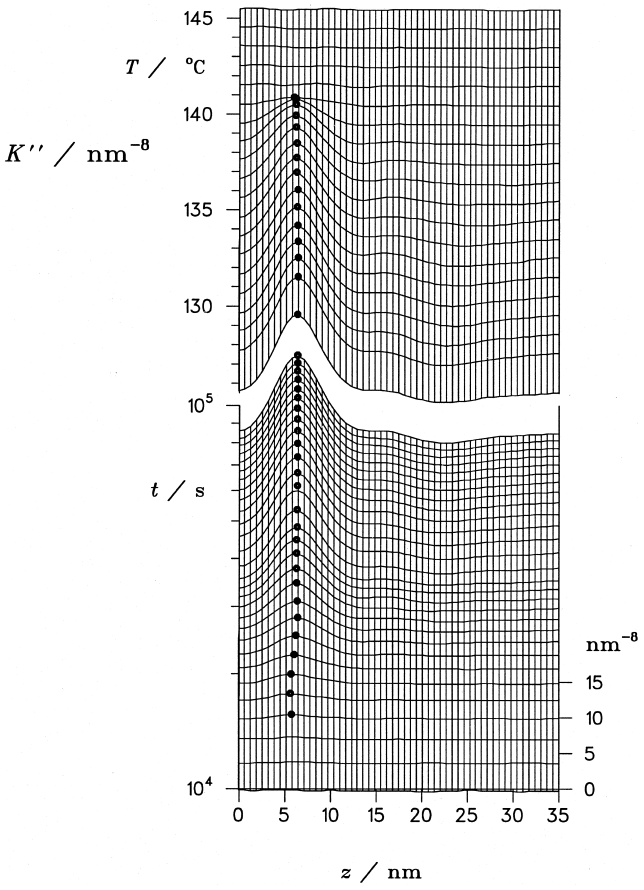

Fig. 1. s-P(P-*co*-O)4: changes of the interface distance distribution function $K''(z)$ during an isothermal crystallization at 125.5°C (bottom) and a subsequent heating up to the melt (top). Curves are vertically shifted by amounts which increase linearly with time or temperature. Counting times for each SAXS curve were 1800 and 3600s; the times at $z = 0$ are the times in the center of the measuring intervals.

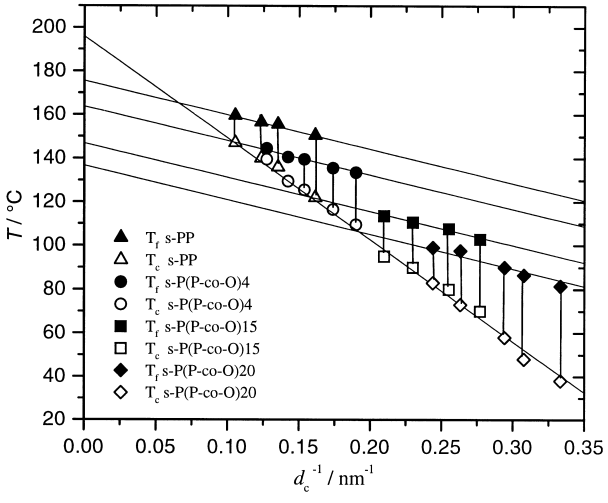

Fig. 2. s-PP and s-P(P-*co*-O)*x*: crystallization line T_c versus d_c^{-1} (open symbols) and Gibbs–Thomson melting lines T_f versus d_c^{-1} (filled symbols) as derived from time- and temperature dependent SAXS experiments.

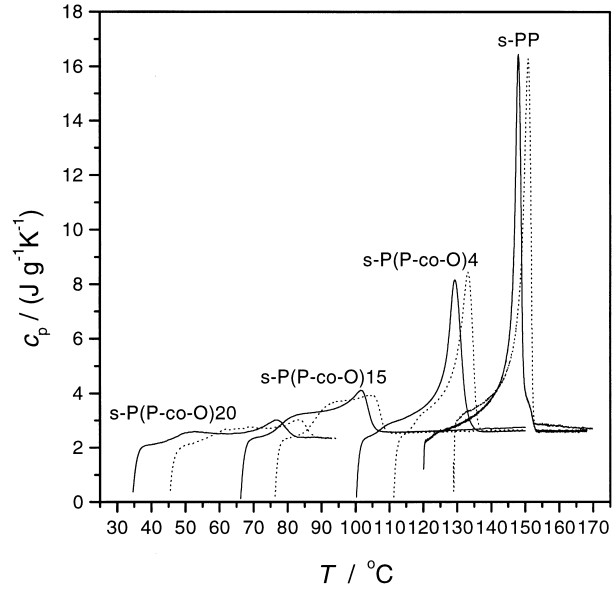

Fig. 3. s-PP and s-P(P-*co*-O)*x*: DSC thermograms measured for the different samples subsequent to isothermal crystallizations (heating rate: 10 K min^{-1}). Two curves, a linear and a dotted one, are displayed for each sample.

at T_f. Stabilization takes place at constant d_c. Many of the crystallites reach the highest perfection, i.e. melt at T_f, but for others there is no or only a partial stabilization and they melt earlier.

1.2. The new questions

We thus have a clear scenario and it leads us to several new questions:

- What is the structural background of the crystallization line?
- Which is the stabilization process transferring the initial imperfect form into the final lamellar crystallites?
- Which mechanism selects d_c and why is it independent from the fraction of non-crystallizable units?
- Are the findings specific for s-PP?

To first answer the last question we carried out an analogous series of experiments on other systems, starting with two poly(ethylene-*co*-octene)s and poly(ϵ-caprolactone). As will be shown, the main features of the s-PP scenario are found again in both systems.

So far the focus of the studies was on the crystal thickness only. Of equal importance, is a knowledge of the crystallinities and their dependence on crystallization temperature and co-unit content. We therefore complemented our studies on s-PP and determined crystallinities for the polyethylenes and poly(ϵ-caprolactone).

In this contribution we describe and discuss our findings in a shortened form. The complete treatments are presented elsewhere [1–3].

2. Experimental

Samples were obtained from the following sources

- The syndiotactic polypropylene (s-PP) and the derived syndiotactic poly(propene-*co*-octene)s (s-P(P-*co*-O)*x*), were synthesized by Jüngling in the Institute of Macromolecular Chemistry of our university, using a metallocene catalyst [4]; samples possess a high stereoregularity, including only 3% of meso diads
- The two poly(ethene-*co*-octene)s (P(E-*co*-O)*x*) of the metallocene catalyst type were supplied by Dow Chemicals Europe
- The sample of poly(ϵ-caprolactone) (PCL) was purchased from Aldrich Chemical Co.

Properties of the samples are given in Ref. [3].

2.1. Instrumentation

The SAXS experiments were carried out with a Kratky-camera attached to a conventional Cu-K_α X-ray source, employing a temperature controlled sample-holder. Using a position-sensitive metal wire detector, scattering curves were usually registered within a few minutes counting time. Complementing the SAXS measurements, crystallinities reached at the end of the isothermal crystallization processes were also determined by differential scanning calorimetry (Perkin–Elmer Model DSC4) and with a mercury filled dilatometer.

For a direct view on the structures we used an atomic force microscope ('Nanoscope III'), employing the tapping technique, thus probing the viscoelastic properties of the surfaces and edges of the crystallites. Samples of s-PP with planar surfaces were prepared in two ways. Films sandwiched between two glass-slides were isothermally crystallized, quenched and placed in ice water, which led to a detachment of one of the glasses. Alternatively we also prepared thin films from spin-coated solutions, which were then melted, isothermally crystallized and quenched.

2.2. SAXS data analysis

Desmeared scattering curves were measured in absolute values as differential cross-sections per unit volume $\Sigma(q)$. With a knowledge of $\Sigma(q)$ the one-dimensional electron density auto correlation function $K(z)$ and its second derivative $K''(z)$, giving the interface distance distribution function [5,6], can be directly calculated by applying the Fourier relations

$$K(z) = \frac{1}{r_e^2}\frac{1}{(2\pi)^3}\int_0^\infty \cos qz \cdot 4\pi q^2\, \Sigma(q)\, \mathrm{d}q \quad (1)$$

and

$$K''(z) = \frac{2}{r_e^2(2\pi)^2}\int_0^\infty [\lim_{q\to\infty} q^4\Sigma(q) - q^4\Sigma(q)] \cos qz\, \mathrm{d}q \quad (2)$$

Here, q denotes the scattering vector $q = 4\pi \sin\theta_B/\lambda$ (θ_B: Bragg scattering angle); r_e is the classical electron radius. In all the measurements the crystal thickness d_c was derived from the location of the respective peak in $K''(z)$.

SAXS experiments enable the crystallinity to be determined. One obtains the 'linear crystallinity' as

$$\phi_1 = \frac{B}{Q+B} \quad (3)$$

Here, $-B$ denotes the ordinate of the 'base line' of $K(z)$ ([7], p. 411) and Q is the integral scattering power identical with $K(z=0)$. ϕ_1 describes the volume fraction occupied by the crystalline lamellae within one stack.

When the sample is densely filled with stacks of laterally extended lamellae then ϕ_1 equals the volume fraction crystallinity ϕ_v. Deviations can arise mainly for two reasons, both leading to $\phi_v < \phi_l$. First, one may encounter a heterogeneous situation, for example, when spherulites fill a sample only partially. Second, the lamellae, although existing as laterally extended objects, may include a certain portion of non-crystalline material between crystalline blocks. If the thickness of the separating regions is below 2 nm there is no scattering effect in the small angle range. It results just in a decrease of the contrast between the layer-like objects with reduced crystallinity and the intervening fully amorphous regions.

3. Results

3.1. Poly(ethylene-co-octene)s

Time- and temperature-dependent SAXS experiments were carried out for two poly(ethylene-*co*-octene)s with 7.5 and 14% per weight of co-units (corresponding to 2 and 4 mol% of octene). Fig. 4 shows as an example the *t*- and *T*-dependence of $K''(z)$ during an isothermal crystallization of P(E-*co*-O)7 at 103°C and a subsequent heating up to the melt. The appearance is similar to Fig. 1: d_c remains constant during both the crystallization process and the subsequent heating, apart from a small increase at the highest temperatures. Fig. 5 collects all data thus obtained for the two samples, again in plots of T_c and T_f versus d_c^{-1}. As for the s-PPs, we find for both samples separate crystallization- and melting lines. The crystallization lines are well defined, but, different from s-PP, there is a slight shift between the two copolymers. Compared to the shift of the melting lines it is still small. While the melting line for P(E-*co*-O)14 is nicely fixed by the data, the melting points obtained for P(E-*co*-O)7 cover a too narrow range to reliably determine the line. The results for the copolymerized s-PPs, where we found a constant slope independent of the co-unit fraction, suggest having the same invariance also for the PEs. In fact, this choice makes sense. As the ratio of the co-unit contents of the two samples is equal to two we can obtain the melting line of perfect polyethylene by repeating the shift upwards,

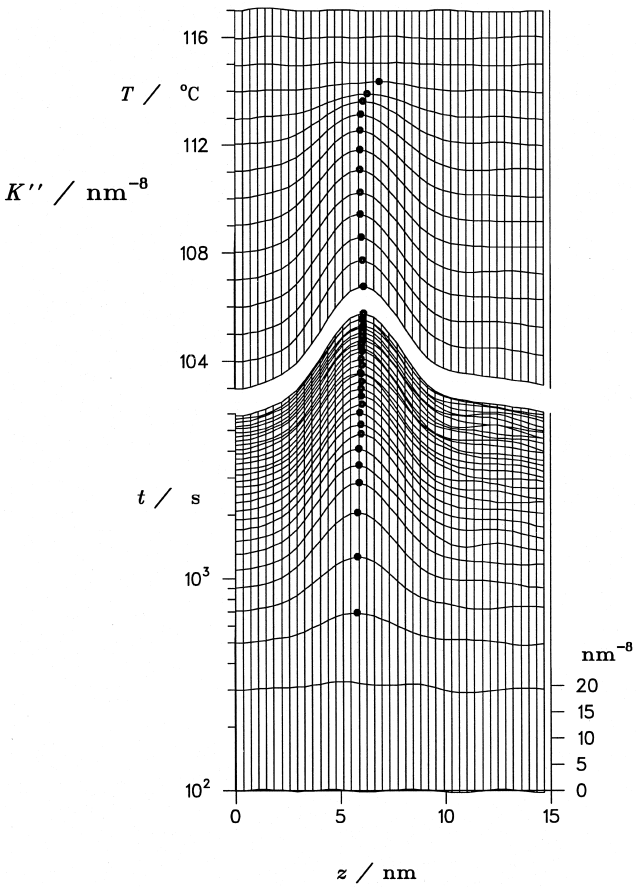

Fig. 4. P(E-*co*-O)7: changes of $K''(z)$ during an isothermal crystallization at 103°C and a subsequent heating up to the melt.

and this extrapolated line is also included in the figure. It indeed starts from 145°C, near the equilibrium melting point of polyethylene. Importantly, the crystallization lines clearly point towards a higher value. Note that this value is in the range where one finds for constrained fibers of high molecular weight PE the transition from the orthorhombic to the hexagonal phase [8]. We deliberately investigated copolymerized polyethylene with large side groups rather than the homopolymer, because the behavior of the latter is complicated by superposed solid-state thickening processes. As a result, a broad distribution of crystal thicknesses arises, which changes with time and temperature, and then it is impossible to determine the original thicknesses giving the crystallization line. For the copolymers the intracrystalline sliding processes are suppressed and the crystal thickness becomes fixed.

3.2. Poly(ϵ-caprolactone)

Fig. 6 presents the structure evolution of poly(ϵ-caprolactone) during an isothermal crystallization at 40°C and the subsequent heating up to 60°C in the molten state. The dominating peak is due to the crystallites. They have a thickness of 6.8 nm at this temperature, with a distance $L = 15$ nm between neighbors. There is no crystal thickening during the crystallization and only a slight shift of the maximum at the end of the heating process. Experiments therefore yield again accurate results with regard to the dependencies between T_c, d_c and T_f. The relations are shown in Fig. 7. Data determine the Gibbs–Thomson melting line and lead again to a linear relation between d_c^{-1} and T_c, i.e. a well defined crystallization line. One observes a large difference between the limiting temperatures of the crystallization and the melting line. For crystallization temperatures below 40°C one observes during heating more pronounced peak shifts, as is indicated by the curved lines connecting the points obtained at the begin and the end of heating.

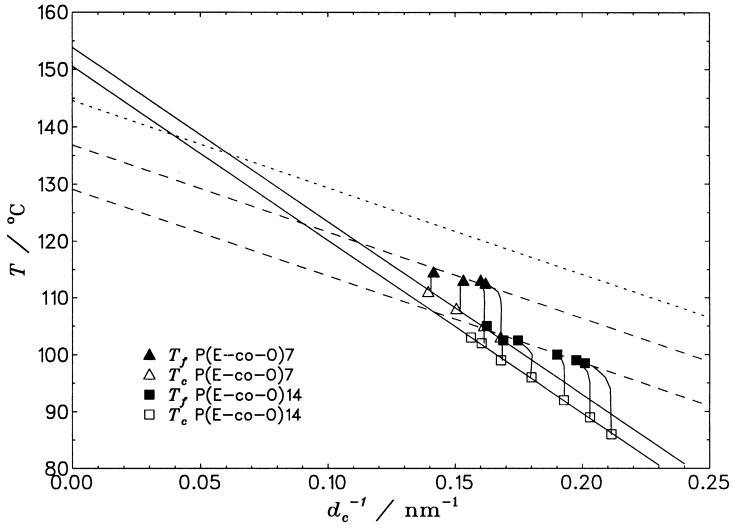

Fig. 5. P(E-*co*-O)*x*: crystallization lines T_c versus d_c^{-1} (open symbols) and melting lines T_f versus d_c^{-1} (filled symbols) as derived from time- and temperature dependent SAXS experiments. The dotted line is the extrapolated melting line of linear polyethylene.

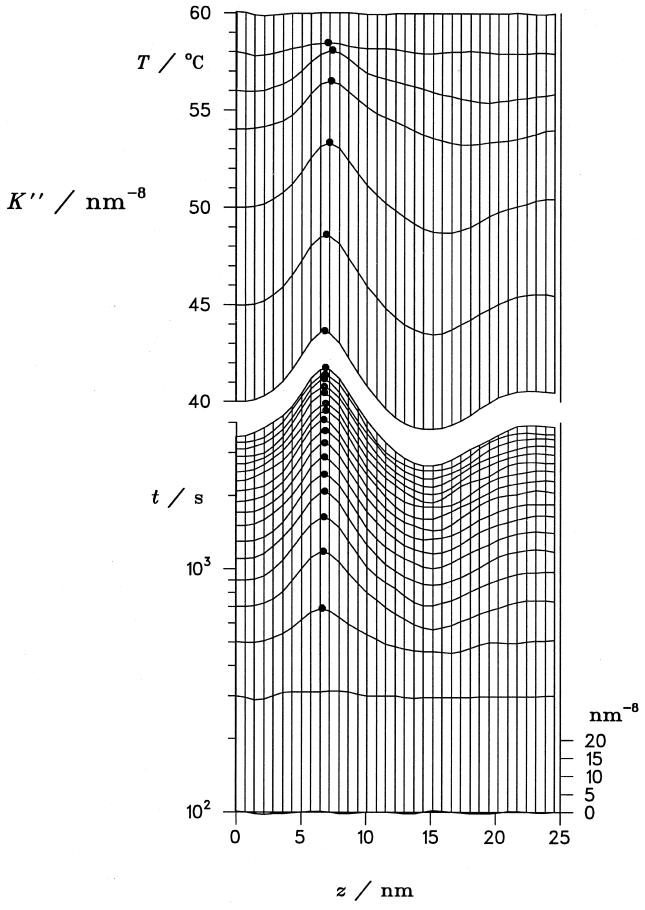

Fig. 6. PCL: changes of $K''(z)$ during an isothermal crystallization at 40°C and a subsequent heating up to the melt.

3.3. Crystallinities after isothermal crystallizations

Fig. 8 shows for all investigated s-PP based samples the crystallinities after complete isothermal crystallization when determined directly at the various T_cs, i.e. without cooling to room temperature. Both, the linear crystallinities deduced from the SAXS data and the weight fraction crystallinities derived from DSC melting curves are given. The overall result is surprisingly simple: For each sample the crystallinity is invariant over the range of accessed T_cs. This seems to be true for both, the linear crystallinity ϕ_1 and the weight fraction crystallinity ϕ_w, with the exception of the highest T_cs chosen for the two copolymers with the highest co-unit contents. Comparison of ϕ_1 and ϕ_w shows a clear tendency: There seems to be a perfect agreement for s-PP, but then, rather than finding $\phi_w > \phi_1$ as expected for a sample completely filled with stacks of laterally extended crystallites, one always observes $\phi_w > \phi_1$. The ratio ϕ_w/ϕ_1 decreases with increasing content of co-units. The figure includes also the temperature dependence of the crystal thickness, just to show the difference in behavior. While the crystallinity remains constant for each sample one finds always distinct changes in the crystal thickness. The result implies that crystal thickness and long spacing vary proportional to each other. A change of the crystallization temperature modifies the length scales of the partially crystalline structure, but has no effect on the global fractions of the crystallized and non-crystallized chain parts.

Fig. 9 shows the results of analogous measurements on the poly(ethylene-*co*-octene)s. To have control about possible long-time perfectioning processes we here used dilatometry. Although the values of ϕ_1 show some scatter there is

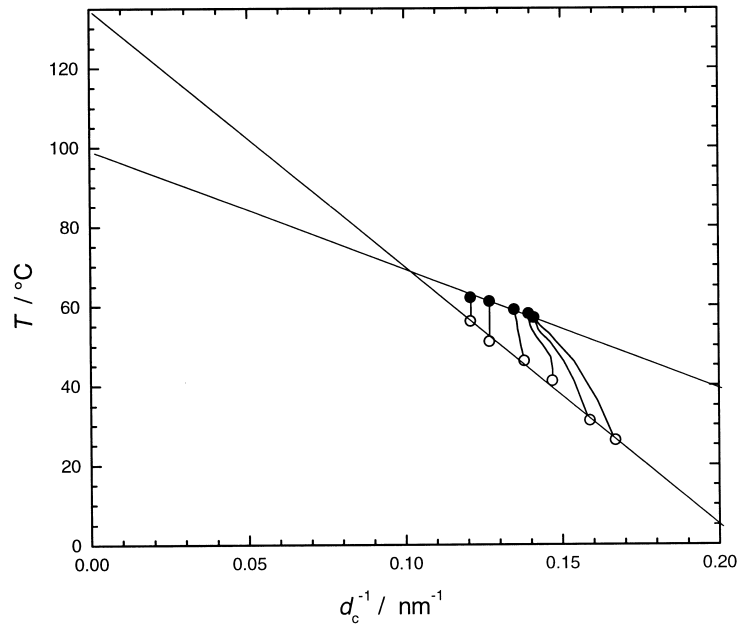

Fig. 7. PCL: crystallization line T_c versus d_c^{-1} (open symbols) and melting line T_f versus d_c^{-1} (filled symbols) as derived from time- and temperature dependent SAXS experiments.

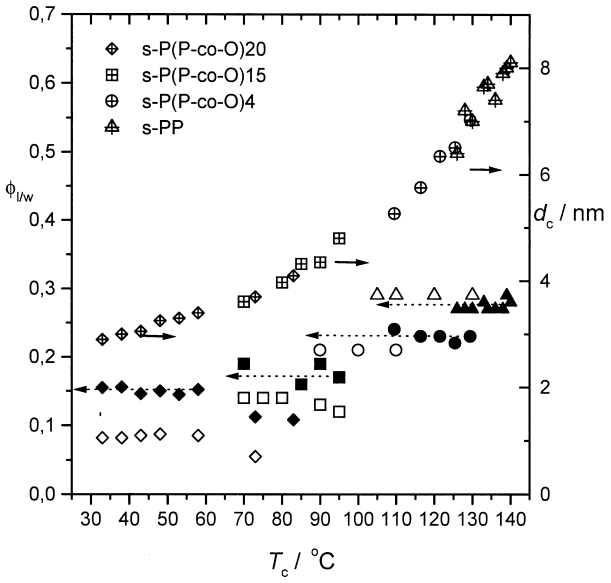

Fig. 8. Crystallinities of s-PP and s-P(P-*co*-O)*x* after isothermal crystallizations at different T_cs: weight fraction crystallinity ϕ_w derived from the DSC signal (open symbols) and linear crystallinity ϕ_l deduced from $K(z)$ (filled symbols). The T_c-dependence of d_c is shown for comparison (right axis).

clearly no tendency for a change with T_c, at least when comparing it to the distinct changes in d_c. For the sample with the lower octene content the weight fraction crystallinity corresponds to the linear crystallinity, for the sample with the higher co-unit content we again find $\phi_w < \phi_1$. In tendency, the ratio ϕ_w/ϕ_1 decreases with T_c, similar to s-P(P-*co*-0)20.

Finally, Fig. 10 shows the crystallinities of poly(ϵ-caprolactone) after the various isothermal crystallization processes, again in a comparison to the temperature dependence of the crystal thickness. The linear crystallinity ϕ_1 is again constant. Values of ϕ_w were obtained by DSC and therefore only in a limited temperature range. Over this range we have good agreement with ϕ_1, as is indicative for a sample densely filled with stacks of laterally extended lamellae.

4. Discussion

The results obtained for the two ethylene-octene copolymers and poly(ϵ-caprolactone) demonstrate that the main conclusions derived from the previous studies on the s-PP based materials are not peculiar but generally valid. In all the cases studied, the transformation of the melt into the partially crystalline state is a two-step process, beginning with the formation of a well-defined initial structure with lower order, which is subsequently stabilized to end up in the final state with layer-like morphology. The signature of the initial state is the crystallization line d_c^{-1} versus T_c, that of the final state the Gibbs–Thomson melting line d_c^{-1} versus T_f. Stabilization is basically achieved without any detectable change in d_c. For a larger part the stabilization is complete, which is indicated by a melting at T_f, in other regions it remains incomplete as is indicated by an earlier melting. The respective weights change with the co-unit content. The higher the fraction of co-units, the more the stabilization is hindered, and the larger is the part which remains in the initial stage.

The crystallization line and the melting line determine together the range of accessible partially crystalline states. The d_c^{-1}/T-phase diagram provides an appropriate description

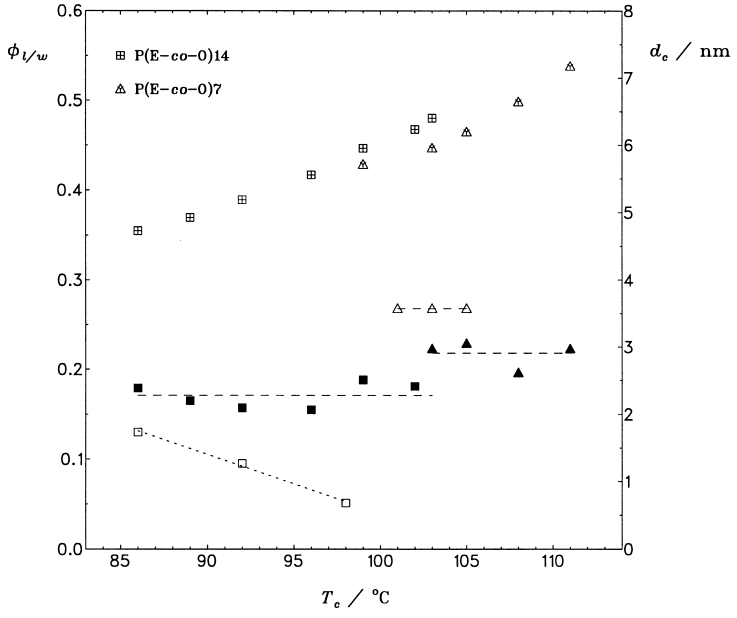

Fig. 9. Crystallinities of P(E-*co*-O)*x* after isothermal crystallizations at different T_cs: weight fraction crystallinity ϕ_w derived from the dilatometric curves (open symbols) and linear crystallinity ϕ_l deduced from $K(z)$ (filled symbols). T_c-dependence of d_c (right axis).

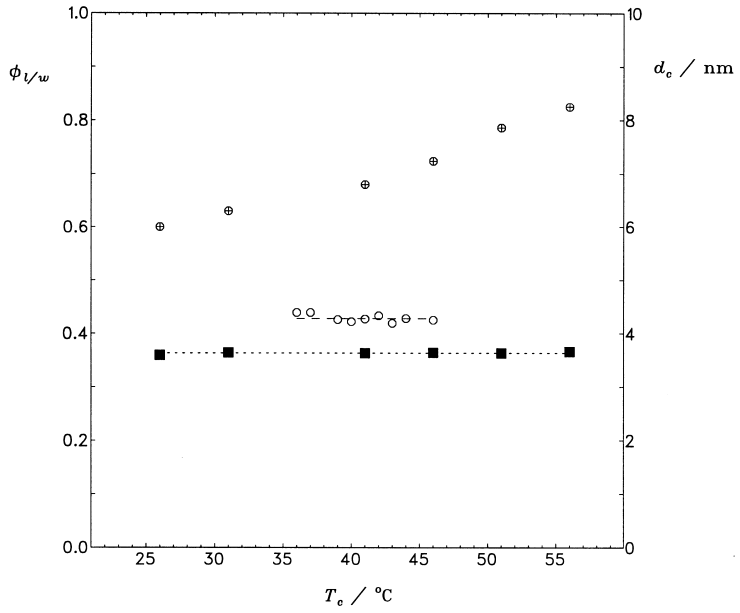

Fig. 10. Crystallinities of PCL after isothermal crystallizations at different T_cs: weight fraction crystallinity ϕ_w derived from the DSC signal (open symbols) and linear crystallinity ϕ_l deduced from $K(z)$ (filled symbols). T_c-dependence of d_c (right axis).

and Fig. 11 presents the general situation in a schematic drawing. All the accessible states are contained in the filled range bounded by the two lines. Its extension is determined by the slopes of the two lines and their limiting temperatures T_f^∞ and T_c^∞. In principle all states below the Gibbs–Thomson melting lines are thermodynamically stable, but obviously, due to the peculiar mechanism of the transition from the melt into the partially crystalline state, not accessible throughout.

Note that it is T_{cf} which is usually obtained by the popular Hoffman–Weeks-plots, rather than the equilibrium melting point as is erroneously assumed by many authors. Errors resulting from this incorrect assignment can be drastic. For example, for the PCL sample the equilibrium melting point, as derived from the melting line when extrapolated to $d_c^{-1} = 0$, is located around 100°C rather than 70°C, as given in the literature based on an application of the Hoffman–Weeks procedure.

Hints at the structural character of the initial form come from electron micrographs of other semi-crystalline polymers. There are indications for a granular substructure of the lamellae, which sometimes resemble planar arrays of blocks rather than being continuous. This was directly observed by Kanig during the initial stage of crystallization of linar

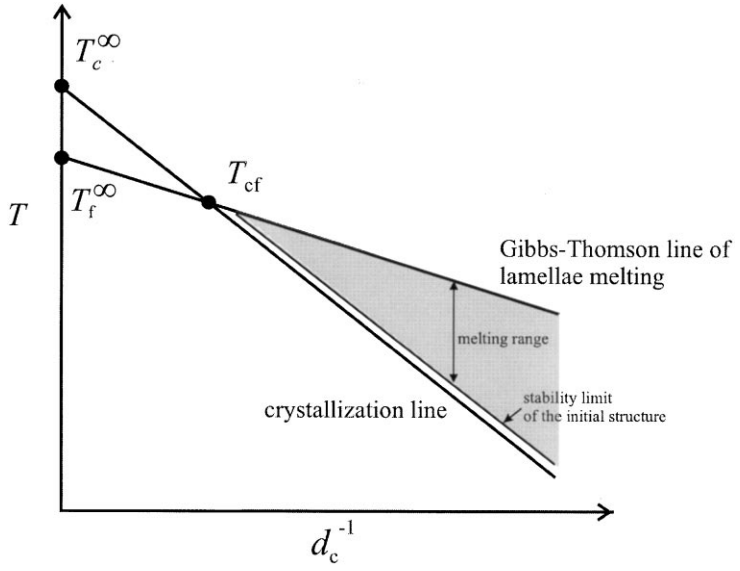

Fig. 11. Schematic of d_c^{-1}/T-diagram of partially crystalline states.

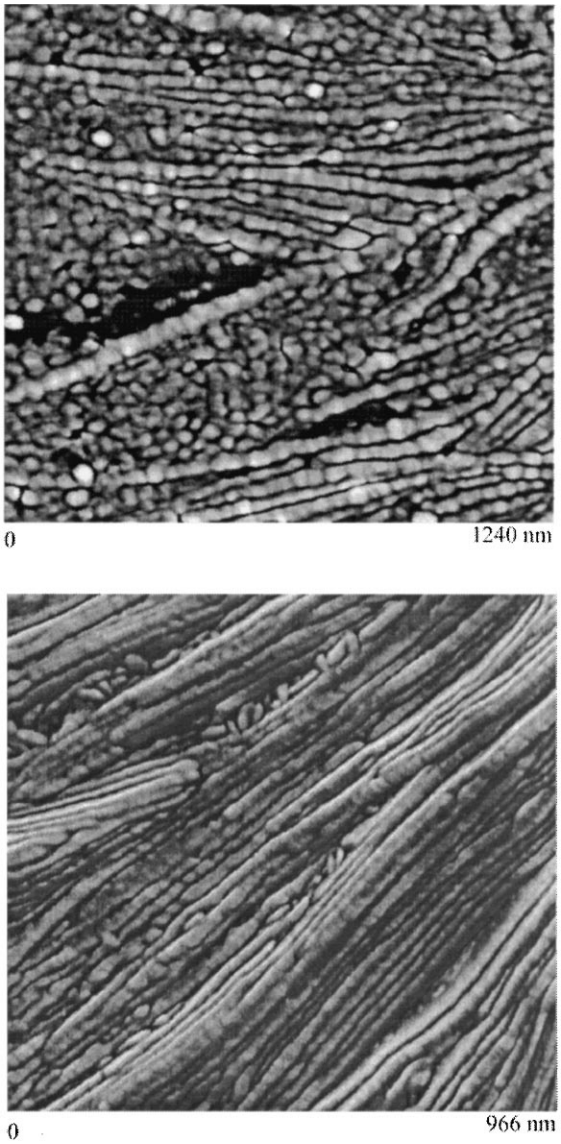

Fig. 12. s-PP, isothermally crystallized at 135°C (top) and subsequently annealed at 150° (bottom). Tapping mode AFM phase image.

polyethylene [9], or indirectly by Bassett and Patel [10] for poly(4-methylpentene-1), where the melting of the subsidiary crystallites occurs at single sites, as if individual blocks became unstable. In addition, for blocks one expects a particularly strong effect of the size on their stability limit, as it becomes apparent in the large slope of the crystallization line.

We further checked this view, in an AFM-investigation of s-PP.Fig. 12 shows two images obtained with the Nanoscope III employing the tapping technique. The upper micrograph was obtained after a crystallization at 135°C. Contrasting all known TEM pictures, which show planar lamellae, here a granular substructure shows up. Interestingly, the appearance changes on annealing. The lower micrograph was obtained after annealing the sample at a temperature just below the final melting point. Now one has essentially flat lamellae; the substructure has disappeared.

Hence, it looks quite reasonable, to associate the first step in the crystallization process with the formation of crystal blocks. One could speculate that the crystallization occurs by the following sequence of steps. At first, blocks form in a pre-oriented zone of limited thickness which stretches along the growth face. This is indicated by the limiting temperature T_c^{∞} found for the PEs (Fig. 5)which agrees with the known temperature of the orthorhombic-hexagonal phase transition. The blocks aggregate into homogeneous lamellae, and it is this process which provides the stabilization. It takes place without a change in d_c. For higher contents of non-crystallizable units these may accumulate at the lateral faces of the blocks and thus hinder the merging. In this case the blocks melt already shortly above T_c.

The latter observation gives us the selection rule for d_c: At each chosen T_c the blocks have the size which keeps them just stable, i.e. they are near to the limit of their stability. The independence of d_c from the co-unit content could either indicate that the co-units are already shifted away when forming the pre-oriented transition zone, or that the stability limit corresponds to an intrinsic breakdown of the crystalline order rather than resulting from a melting from the surfaces. The suggested scheme implies that the first step in the building-up of polymer crystallites is a cooperative one, being given by the formation of blocks of minimum size. The idea is not as unusual as it might look at first, considering that the reordering of a protein after a denaturation also begins with the formation of small ordered zones which are subsequently attached to a growing central part [11].

The picture of a granular substructure of the lamellae agrees with the observed crystallinities ϕ_w and ϕ_l given in Fig. 8. We find for s-P(P-*co*-0)20 a large difference between the two values, with $\phi_v < \phi_w < \phi_l$, as it should indeed be the case if the layer-like objects producing the scattering are blocks being arranged on planes. When including a dilatometric measurement it becomes possible to carry out a rigorous check and a quantitative analysis. After completion of an isothermal crystallization at 58°C we obtained the following data:

- density increase from dilatometry: $\rho - \rho_a = 0.012\ \mathrm{g\ cm^{-3}}$
- electron density increase from SAXS ([7], p.411): $\sqrt{B} = \rho_e - \rho_{e,a} = 4.4\ \mathrm{nm^{-3}}$
- linear crystallinity from SAXS: $\phi_l = B/(B + Q) = 0.15$

$\rho - \rho_a$ and $\rho_e - \rho_{e,a}$ correspond to each other, since we have generally

$$\rho_e - \rho_{e,a} = \frac{8N_A}{14\ \mathrm{g\ mol^{-1}}}(\rho - \rho_a) \quad (N_A: \text{ Avogadro number})$$

giving $\rho_e - \rho_{e,a} = 4.1\ \mathrm{nm^{-3}}$, in agreement with the SAXS

result within the error limits of the measurements. The agreement can be taken as a proof that the blocks indeed assemble to set up essentially planar objects, as this is the basis for the data analysis via the one-dimensional correlation function.

The blocks do not fill the layers densely. This clearly follows from calculating the difference between the mean electron density of the layers, $\bar{\rho}_{e,c}$, and the amorphous regions, using

$$\bar{\rho}_{e,c} - \rho_{e,a} = \frac{\rho_e - \rho_{e,a}}{\phi_l} = 29.3\ \mathrm{nm}^{-3}$$

This is definitely below the value of the electron density difference between crystalline and amorphous regions [6]

$$\rho_{e,c} - \rho_{e,a} = (29.9 + 0.105\ T[^\circ\mathrm{C})]\ \mathrm{nm}^{-3} = 36\ \mathrm{nm}^{-3}$$

Therefore, the blocks fill the lamellae only to a degree $\phi_{intra} = 29.3/36 = 0.81$, and the global volume fraction crystallinity is $\phi_v = \phi_l \cdot \phi_{intra} = 0.12$.

The finding of a block-like substructure of the lamellae formed in copolymer systems is, of course, not new. They have been repeatedly observed and reported on, maybe for the first time in an early work of Okui and Kawai [12], and, more recently in studies of Minick et al on copolymers of polyethylene, there being addressed as 'beaded strings' [13]. The new insight arises from the combination with the SAXS results. The bare existence of the crystallization line which includes both in common, the nearly perfect s-PP and all the copolymers, clearly indicates that the related initial block dominated structure is *always* formed in the first step, for homo- and copolymers likewise, independent of the final structure reached, which may be composed of homogeneous lamellae, granular lamellae or a mixture of both.

How can the observed constancy of the crystallinity be interpreted? It holds strictly for s-PP, s-P(P-*co*-O)4, P(E-*co*-O)7 and PCL for both ϕ_l and ϕ_w over the whole temperature range covered by the studies. One might feel that the samples with higher co-unit contents, which show a decrease in the crystallinity with increasing temperature, behave in the normal way, in the expected manner. The decrease can be addressed in the spirit of Flory's treatment of copolymer crystallization, as being due to the decrease in the fraction of sequences long enough to build up the crystallites, thereby considering, that in order to remain stable crystal thicknesses must increase with increasing temperature. However, as demonstrated by the results, in the central temperature region and for the majority of studied samples, these ideas do not seem applicable. As a general statement, observations teach us, that the potential of a given polymer system to crystallize is limited and well defined over a larger temperature range. It looks as if the melt would be a two-component fluid, composed of crystallizable and non-crystallizable chain parts with essentially fixed fractions. Indeed, just in recent time evidence is accumulating that supercooled polymer melts may micro-separate into regions with variant properties. These regions may differ in density (Terrill et al., [14]), in the conformational statistics of chains (Tashiro et al. [15]), in the orientational order (Imai et al. [16]), and in their mobility (Fukao and Miyamoto [17]), with indications that the less mobile parts set up a network through the sample (Pogodina and Winter [18]). Typically, these features are only observable during a short period, before the onset of the main part of crystallization, i.e. before the rise of Bragg-peaks in the WAXS diagram. Authors dealing with these phenomena argue, that the establishment of a peculiar kind of order in macromolecular fluids may be due to the high degree of supercooling realized in these systems. Under these conditions one may well envisage spontaneous ordering processes, occurring in an easy way without having to overcome a large activation barrier.

5. Conclusion

Our findings may be summarized as follows:

- The SAXS experiments show the existence of a crystallization and a melting line as two independent features. Consequently, the formation of the semicrystalline state must be a two-step process, beginning with the formation of an initial state of lower order which then passes over into the final lamellar structure.
- The limiting temperature T_c^∞ of the crystallization line

$$T_c = T_c^\infty - C_l d_c^{-1} \tag{4}$$

  which describes the relationship between the crystallization temperature and the crystal thickness is not, or only weakly dependent on the co-unit content. The equilibrium melting point of a sample following from the Gibbs–Thomson melting line

$$T_f = T_f^\infty - C_2 d_c^{-1} \tag{5}$$

  is always below T_c^∞

$$T_f^\infty < T_c^\infty \tag{6}$$

- Investigations with AFM in combination with the SAXS experiments indicate that the initial state is constituted of crystal blocks in planar assemblies.
- Crystallinities remain invariant over larger temperature ranges.

Acknowledgements

Support of this work by the Deutsche Forschungsgemeinschaft (Graduiertenkolleg 'Strukturbildung in Makromolekularen Systemen') is gratefully acknowledged. Thanks are also due to the Fonds der Chemischen Industrie for additional help.

References

[1] Hauser G, Schmidtke J, Strobl G. Macromolecules 1998;31:6250.
[2] Hugel T, Strobl G, Thomann R. Acta Polym 1999;50:214.
[3] Heck B, Hugel T, Iijima M, Sadiku E, Strobl G. New J Phys 1999;1:17.
[4] Thomann R, Wang C, Kressler J, Jüngling S, Mülhaupt R. Polymer 1995;36:3795.
[5] Ruland W. Colloid Polym Sci 1977;255:417.
[6] Schmidtke J, Strobl G, Thurn-Albrecht T. Macromolecules 1997; 30:5804.
[7] Strobl G. The physics of polymers. Berlin: Springer, 1997.
[8] Tsubakihara S, Nakamura A, Yasuniwa M. Polym J 1996;28:489.
[9] Kanig G. Colloid Polym Sci 1991;269:1118.
[10] Bassett DC, Patel D. Polymer 1994;35:1855.
[11] Ptitsyn OB. Adv Protein Chem 1995;47:83.
[12] Okui N, Kawai T. Makromol Chem 1972;154:161.
[13] Minick J, Moet A, Hiltner A, Baer E, Chum SP. J Appl Polym Sci 1995;58:1371.
[14] Terrill NJ, Fairclough PA, Towns-Andrews E, Komanschek BU, Young RJ, Ryan AJ. Polym Commun 1998;39:2381.
[15] Tashiro K, Sasaki S, Gose N, Kobayashi M. Polym J 1998; 30:485.
[16] Imai M, Kaji K, Kanaya T, Sakai Y. Phys Rev B 1995;52:12 696.
[17] Fukao K, Miyamoto Y. Phys Rev Lett 1997;79:4613.
[18] Pogodina NV, Winter HH. Macromolecules 1998;31:8164.